

Time Dependent Hadronization via HERMES and EMC Data Consistency

K. Gallmeister* U. Mosel

Institut für Theoretische Physik, Universität Giessen, Germany

Abstract

Using QCD-inspired time dependent cross sections for pre-hadrons we provide a combined analysis of available experimental data on hadron attenuation in DIS off nuclei as measured by HERMES with 12 and 27 GeV and by EMC with 100 and 280 GeV lepton beam energies. We extract the complete four-dimensional evolution of the pre-hadrons using the JETSET-part of PYTHIA. We find a remarkable sensitivity of nuclear attenuation data to the details of the time-evolution of cross sections. Only cross sections evolving linearly in time describe the available data in a wide kinematical regime. Predictions for experimental conditions at JLAB/CLAS (5 and 12 GeV beam energies) are included.

Key words: hadron formation, Lund model, deep inelastic scattering, electro-production, hadron induced high-energy interactions, meson production
PACS: 12.38.Lg, 13.60.-r, 13.85.-t, 25.75.-q, 25.30.c

1 Introduction

The process of hadronization, i.e. the question of how some partonic state evolves into a final observed hadron wave function, is still not understood.

For an understanding of jet interactions in hot and dense (possibly quark-gluon) matter, investigated in ultra-relativistic heavy-ion collisions, or even in cold nuclei, investigated e.g. by the EMC and the HERMES experiments, two main features need clarification: first, the time it takes to form a hadron needs to be known. Here we address the time between the initial interaction until

* Corresponding author.

Email address: Kai.Gallmeister@theo.physik.uni-giessen.de
(K. Gallmeister).

the final on-shell propagation of the produced particle. Second, the question, how this 'unknown object' interacts with the surrounding matter during its 'formation time' has to be answered (1).

Since hadron production in electromagnetic interactions with the nucleon is assumed to be simpler than e.g. the same process in heavy-ion reactions, deep inelastic scattering (DIS) is the process one has to understand first, since here at least the state of the matter in which the parton propagates is known. The essential question then is how long it takes until the field of a knocked-out color charge is rebuilt.

In a classical picture, the distance of two (color-)charges with some transverse momentum $\kappa_T = \sqrt{\langle k_T \rangle^2} \sim 0.35 \text{ GeV}$, initially set to zero, evolves linearly in time. Therefore the cross-section is quadratic in time, $\sigma = \pi r^2 \simeq t^2$. However, any quantum mechanical description has to respect the uncertainty principle. This implies that the assumption of a constant transverse momentum like the above κ_T is not valid: Going to very first stages with $r \rightarrow 0$ leads to $k_T \rightarrow \infty$. A consequent consideration of consecutive transversal weakening leads to a linear time dependence of the cross section, $\sigma \simeq t$, as pointed out by Dokshitzer et al. (2).

The authors of ref. (2) also stressed that the constraints in the above considerations leading to a linear time dependence of the cross section may be weakened by quantum effects resulting from non-vanishing values of the characteristic scales, as e.g. the squared momentum Q^2 in DIS, and as a consequence, the exact time-dependence of the cross section is expected to lie somewhere between linear and quadratic. Experiments should be able to tell which the better time-dependence at a given momentum transfer is (2).

There have already been some studies employing time-dependent cross-sections for the description of final state interactions in ultra-relativistic heavy-ion collisions (3; 4). Such studies, however, introduce as already mentioned another unknown into the analysis, the properties of the matter surrounding the formed hadron. Here, in the present paper, we therefore want to use data on nuclear attenuation of hadrons in cold nuclei, obtained by the EMC and HERMES experiments. A similar analysis for quasi-exclusive data (5), which is similar in spirit to ours, suffered from the lack of reliable data at that time.

2 Time Development of Interactions

We first stress that most reactions considered in this paper have relatively small $\langle Q^2 \rangle$ values of only $1 - 2 \text{ GeV}^2$. The applicability of methods of perturbative QCD thus is doubtful. This is the common feature of the HERMES

and JLAB experiments that work in quite different energy regimes. It is thus desirable to develop a description that works for all three energy regimes and describes the transition from high energies to low energies correctly. Our model of reactions on nuclei relies on a separation of processes: In step 1) the beam lepton interacts with a nucleon. This is modeled via the PYTHIA (7) event generator assuming that this interaction with nucleons in a nucleus is the same as that on a free proton/neutron. We do, however, take into account nuclear effects like Fermi motion, Pauli blocking and nuclear shadowing (for details see (8; 9; 10)).

The PYTHIA model used for step 1) has been proven to be very successful in describing hadron multiplicities, momentum distributions etc. in many kinds of interactions, also at the low Q^2 and ν values considered in this paper. The model combines hard physics for the initial parton interactions and soft physics in modeling the fragmentation function. We have therefore used PYTHIA as our major source of information about the underlying process of fragmentation. The extraction of the space-time production and formation points from PYTHIA is described in (11). Contrary to many analytic estimates of formation times, we extract our information per particle per event during our Monte Carlo simulations and do not use any averaged distributions. There is thus no longer any freedom in choosing the relevant times in our approach. We note that these times are model dependent, since they rely on the Lund string fragmentation picture as implemented in PYTHIA. However, the simultaneous analysis of attenuation data on various targets may help to separate effects of times from those of pre-hadronic interactions. We also stress that PYTHIA not only contains string fragmentation, but also direct interaction processes such as diffraction and vector meson dominance.

As elaborated in (11), in every event during the Monte Carlo calculations and for each final particle we extract three 4D-points in PYTHIA: First, for example, the two production points $P1$ and $P2$ of the quark and antiquark that make up a final meson; these are the points where the string breaks occur for each of the two quarks. The meeting point of the quark lines starting at these two production points is identified with the hadron formation point (denoted by F). The corresponding “formation time” is denoted by t_F .

In the following we will always identify the “production time” of a particle with the “first” string break, i.e. $t_P = \min(t_{P1}, t_{P2})$. We have checked that our results are frame independent: Doing the time ordering in the laboratory frame or in the center of momentum frame of the string has no influence.

Resulting directly from the fragmentation, any meson or baryon may consist of 0, 1, 2 or even 3 (“leading”) partons, which build up the initial string configurations. “Leading” particles have at least one parton line directly connected with the hard interaction point and also have at least one production

time which is zero in all frames. Their properties are, therefore, directly determined by the Q^2 of the primary virtual photon. Particles with 0 leading partons, i.e. “secondary” or “non-leading” particles, all have non-vanishing production times (as described in ref. (11) both production points are different from the hard interaction point). We note that this picture is very similar to that proposed by Kopeliovich et al. (1; 12).

While so far we have used only well tested in vacuo descriptions of particle production, we now model in step 2) the in-medium changes of the fragmentation function by introducing (pre-)hadronic interactions between the production and the formation times. In this step 2) all produced (pre-)hadrons are propagated through the surrounding nuclear medium according to a semiclassical Boltzmann–Uehling–Uhlenbeck (BUU) transport description which allows for elastic and inelastic rescattering and side-feeding through coupled-channel effects. For details we refer the reader to (8; 9; 10). For the actual numerical treatment of final state interactions we have used the completely rewritten, new GiBUU code (13), which is based on the theory and methods described in (8; 9; 10) and reproduces the results presented there.

In this work we will consider four different time evolutions for the cross sections between the production time t_P and the formation time t_F ; after t_F the hadrons interact with their full cross section. In the first scenario we assume no time dependence at all, i.e. the pre-hadronic cross section is constant,

$$\sigma^*/\sigma = const = 0.5 \quad , \quad (1)$$

where σ is the full hadronic cross section. Here the value 0.5 for the constant cross section ratio is chosen because it gives a reasonable description of the HERMES data (10). The next two scenarios are the “quantum mechanically inspired” and the “naive” assumptions of linear or quadratic increase, respectively

$$\sigma^*(t)/\sigma = \left(\frac{t - t_P}{t_F - t_P} \right)^n \quad , \quad n = 1, 2 \quad . \quad (2)$$

All three scenarios for the pre-hadronic interaction mimic to some extent color transparency because the interaction rates are reduced until the formation of the final hadron.

Finally, we implement the ‘quantum diffusion’ picture of Farrar et al. (5) proposed by these authors to describe the time-development of the interactions of a point-like configuration produced in a hard initial reaction (see also (6)). This picture combines the linear increase with the assumption that the cross section for the *leading* particles does not start at zero, but at a finite value connected with Q^2 of the initial interaction,

$$\sigma^*(t)/\sigma = X_0 + (1 - X_0) \cdot \left(\frac{t - t_P}{t_F - t_P} \right) \quad , \quad X_0 = r_{\text{lead}} \frac{\text{const}}{Q^2} \quad , \quad (3)$$

with r_{lead} standing for the ratios of leading partons over the total number of partons (2 for mesons, 3 for baryons). The baseline value X_0 is inspired by the coefficient $\langle n^2 k_T^2 \rangle / Q^2$ in (5). Our scaling with r_{lead} guarantees that summing over all particles in an event, on average the prefactor becomes unity. The numerical value of the constant in the numerator of X_0 is chosen to be 1 GeV² for simplicity, close to the value used in (5). This value is also constrained by the considered Q^2 range such that the pedestal value $X_0 \leq 1$ is fulfilled. In all four scenarios the (pre-)hadronic cross section is zero before t_P and equals the full hadronic cross section after t_F . The most essential feature of color transparency – larger hadrons (smaller Q^2) get attenuated more than smaller ones – is thus included in all four scenarios. Until the hadron reaches its physical groundstate the actual cross section will oscillate around an average as pointed out by Kopeliovich et al. (14).

It is worthwhile to reemphasize the differences of the cross section evolutions of leading and non-leading particles in the last model: *leading* particles start to interact with a non vanishing (i.e. a pedestal) cross section at the hard interaction time; they 'remember' the Q^2 of the incoming photon. *Non leading* particles are entirely generated by soft string breaks, they are detached from the hard interaction point and have no memory of the original hard interaction process. They, therefore, start to interact at later times with zero cross section. In both cases, the cross section increases with time. These features reflect color transparency.

In contrast to other descriptions of the attenuation of jets in photonuclear reactions (1; 12; 15) our method describes the whole kinematical range of final particles and is thus not restricted to leading hadrons or very high energies only.

3 Results

In all the following discussions we express the modification of the spectra by the medium via the usual nuclear modification ratio

$$R_M^h(\nu, Q^2, z_h, p_T^2, \dots) = \frac{[N_h(\nu, Q^2, z_h, p_T^2, \dots) / N_e(\nu, Q^2)]_A}{[N_h(\nu, Q^2, z_h, p_T^2, \dots) / N_e(\nu, Q^2)]_D} \quad , \quad (4)$$

where all the hadronic spectra on the nucleus (“A”) as also on deuterium (“D”) are normalized to the corresponding number of scattered electrons. As indicated, the nuclear modification ratio can be displayed as function of many

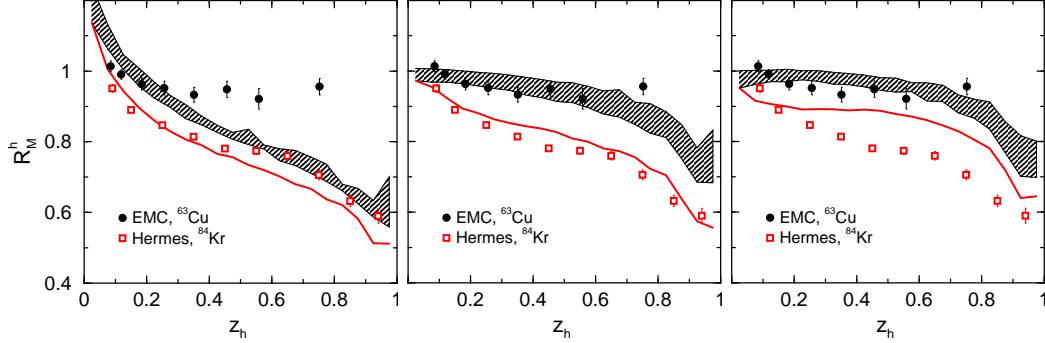


Fig. 1. Nuclear modification factor for charged hadrons. Experimental data are for HERMES@27GeV (16) and EMC@100/280GeV (17). The predictions for the two EMC energies are given by the lower and upper bounds of the shaded band. The cross section-evolution-scenarios in the calculations are: constant, linear, quadratic (from left to right).

variables as e.g. ν , z_h , p_T^2 etc. Most information would be provided by multidimensional distributions, which are, however, not yet available experimentally.

The “photonic” parameters of the collisions are given by ν as photon energy and by Q^2 as the transferred four momentum squared. The third parameter to fix all lepton/photon kinematics is given here by the lepton beam energy.

The “hadronic” variables we focus on in this paper are z_h or p_T^2 . Here z_h stands for the ratio of the energy of the hadron divided by the energy of the photon, while the squared transverse momentum in respect to the photon direction is indicated by p_T^2 .

We emphasize here our earlier findings (10) that the interpretation of the ν dependence of experimental hadron attenuation is complicated by experimental acceptances and integration cuts. These influence the slope of $R(\nu)$ so that a “physical” interpretation is possible only if these experimental acceptance effects are taken into account in the comparison of theory with experiment. Only a full event description such as the one presented here can thus lead to a reliable interpretation of experimental data. In our theory the description of the ν dependence is fixed by the description of the z_h dependence.

In fig. 1 we show for the three scenarios according to eqs.(1),(2) (with $n = 1, 2$) the results of our calculations compared to experimental data (16; 17). Because it remains unclear to us how the (very) different lepton energies were considered in the experimental results given in (17) we have performed the calculations for the two most prominent energies of that experiment, i.e. for beam energies of 100 GeV and 280 GeV. We illustrate the results of our calculations for this experiment by a shaded band in the following figures.

Assuming a constant cross section (leftmost panel in fig. 1), we obtain a good description of the HERMES results, while the attenuation for the EMC experiment is much too strong (cf. (10)). Assuming a linear time dependence, both the HERMES and EMC attenuation are well described¹. Going even further and assuming a quadratic time dependence (rightmost panel in fig. 1), the theoretical attenuation is too weak both for the HERMES and for the EMC experiment, with the discrepancy between theoretical and experimental results being significant for the HERMES experiment. Only the theoretical scenario with a cross section evolving linearly in time (middle panel in fig. 1) is able to describe both data sets at the same time.

In order to understand these findings, we show in fig. 2(a) the averaged production $\langle t_P \rangle$ and formation times $\langle t_F \rangle$ in the target rest frame for the two experimental setups of HERMES@27GeV and EMC@100GeV as results of our MC calculation. In fig. 2(b) we sketch the different evolution scenarios for some

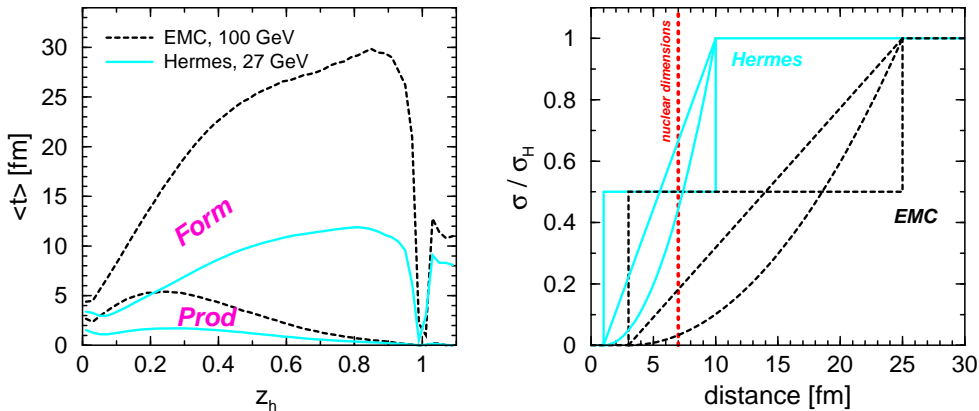


Fig. 2. *Left: averaged production times $\langle t_P \rangle$ and formation times $\langle t_F \rangle$ in the target rest frame for EMC@100GeV and for HERMES@27GeV as a function of z_h (11), averaged over leading ($t_P = 0$) and non-leading ($t_P > 0$) hadrons. The lowest curves give the production times whereas the two upper curves give the formation times for the beam energies indicated. Values of $z_h > 1$ can arise for baryon jets. Right: sketch of the evolution of the (scaled) cross section as function of distance from the interaction point according to scenarios eqs.(1) and (2) (with $n = 1, 2$): constant, linear, quadratic increase. The solid lines give the time-development for the HERMES energy regime, while the dashed lines show that for the EMC regime.*

arbitrary chosen values of production and formation times and compare these with a typical nuclear distance of $\simeq 7$ fm. One sees clearly the different effects that the two scenarios (linear and quadratic rise of cross-sections) have in the two different kinematical regimes. For example, the quadratic scenario leads to nearly zero interaction within the first 7 fm for the EMC energy because at this higher energy the hadron has left the nucleus before the cross section has

¹ Fig.3 in (17) also contains data points leading to $R_h(z_h = 0.9) = 0.83$, which fits very well into the calculated energy-band. This point is not contained in the other figures in that paper and is, therefore, not shown in our fig. 1.

risen to any significant value. On the other hand, for HERMES kinematics the cross section reaches about $0.5 \sigma_H$ in that same distance. Figs. 1 and 2 together show an amazing sensitivity to the different scenarios for the time-dependence of the cross section. Going to lower energies than 27 GeV beam energy (as e.g. with 12 GeV or even with 5 GeV lepton beam energy) results in events, where all the hadronization happens within the nuclear distances; at 5 GeV beam energy the averaged formation time is $\simeq 4$ fm at $z_h \simeq 0.8$. In these cases we lose sensitivity to the pre-hadronic interaction and in particular, to their time-dependence.

Fig. 3 shows results of our calculations employing the scenario as given by eq. 3. While not very pronounced, the effect of the non-vanishing, Q^2 -dependent

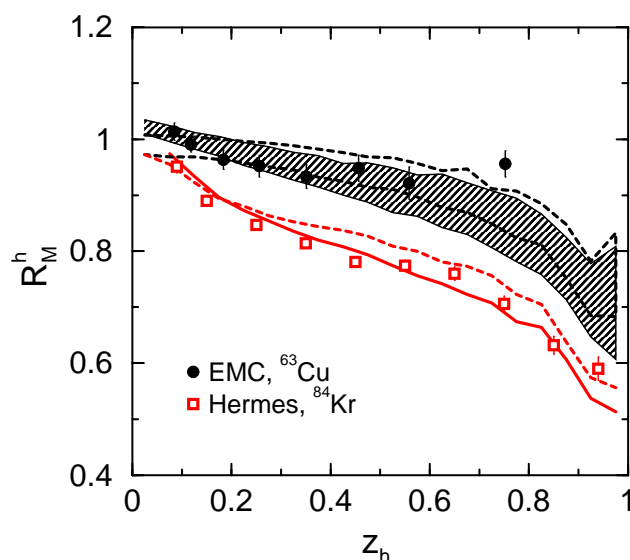


Fig. 3. Nuclear modification factor for charged hadrons as in fig. 1. The cross section evolution-scenario in the calculations is according to eq.(3). Dashed lines repeat curves from fig. 1 (middle panel).

initial cross section of the leading particles is visible when comparing fig. 3 with the middle panel in fig. 1; a slight improvement in the description can be seen. The observed smallness of the Q^2 dependence is in line with experimental observations of both the HERMES and the EMC experiment (16; 17). This scenario (eq. 3) will therefore be the scenario of our choice for the following considerations.

Fig. 4 shows a comparison of our calculations with the latest experimental data of the HERMES collaboration with 27 GeV beam energy for identified hadrons for the four targets ^4He , ^{20}Ne , ^{84}Kr and ^{131}Xe . As expected from fig. 3 for the total hadron yield, the data for pions, that make up most of the produced hadrons, are described very well by our calculations. In the large z_h region charged pions stem mostly from decays of diffractive rhos. Since these pions are taken out from the experimental data, we also switch off diffractive

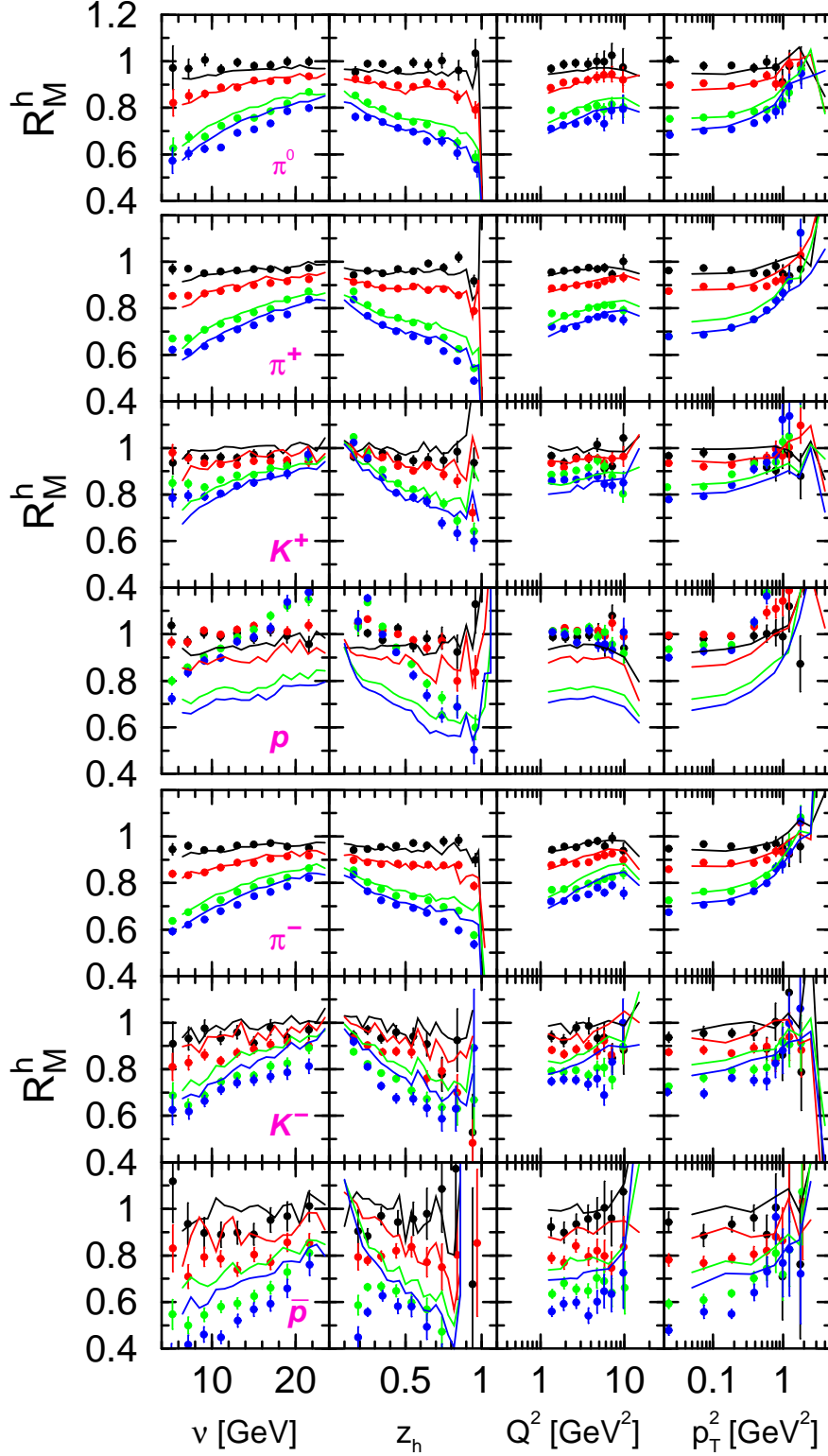


Fig. 4. Nuclear modification factor for identified hadrons for HERMES@27 GeV with ^4He , ^{20}Ne , ^{84}Kr and ^{131}Xe target (top to bottom). Points indicate experimental data (16) while the curves represent our calculations with the time-dependence scenario eq. (3) and diffractive events switched off.

production of rhos in the calculations shown. While the description of the data for the strange and anti-baryonic sector is also quite good, one still sees the well known discrepancy of data and calculations for protons: the regions with “low z_h ”/”high ν ” are clearly underestimated in our model. We recall that this is not a new finding but already known from our previous work (10). The observed discrepancy may reflect a deficiency in our treatment of final state interactions at high proton energies since the (strongly non-perturbative) low- z_h protons arise mainly from energy-degrading rescattering events. The discrepancy may, however, also reflect some problem with the treatment of experimental geometrical acceptance limitations which are contained in the data (and simulated in the calculations).

Fig. 5 shows our model results compared with experimental data of the HERMES Collaboration for the nuclear modification factor of charged hadrons and/or pions on a ^{84}Kr target with the 12 GeV beam. While the inclusive

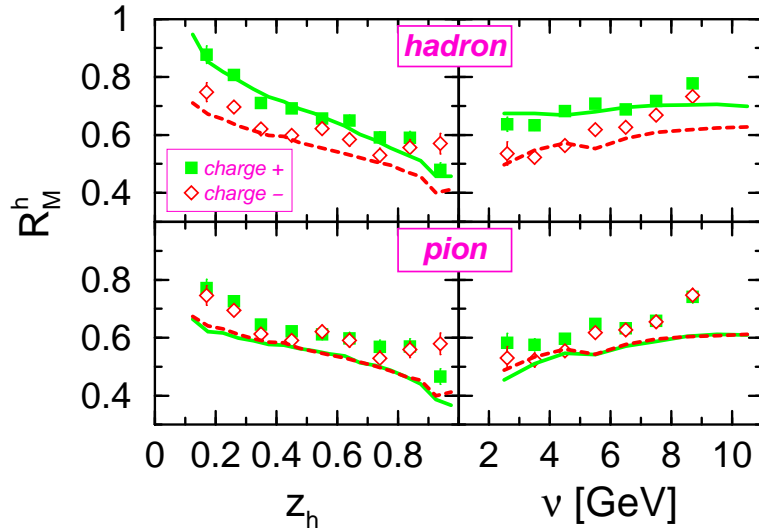


Fig. 5. Nuclear modification factor of charged hadrons/pions for HERMES@12GeV on ^{84}Kr target. The upper panel shows the results for charged hadrons, while the lower panel stands for charged pions only. Charge states are separated: Positive charge (full symbols, straight line) and negative charge (open symbols, dashed lines).

data for both charge states of all charged hadrons are very well described, the attenuation for the charged pions is somewhat overestimated.

For the ^{14}N target all relevant lengths are smaller and all attenuation effects are smaller: all theoretical curves are identical to their experimental data.

Based on our successful description of the experimental data of the HERMES collaboration for 27 GeV and 12 GeV beam energies, we now make predictions for the meson spectra at the presently available 5 GeV lepton beam energy and at the future JLAB facility with 12 GeV. The details of the implementation of the experimental constraints of CLAS into our MC calculations (18) are

described in Sect. 6.4.4 of (10). We note that we have made already earlier such predictions, using constant pre-hadronic cross sections, for the relevant JLAB energies (10; 19).

We start with a discussion of our results for a 5 GeV beam energy in fig. 6. A

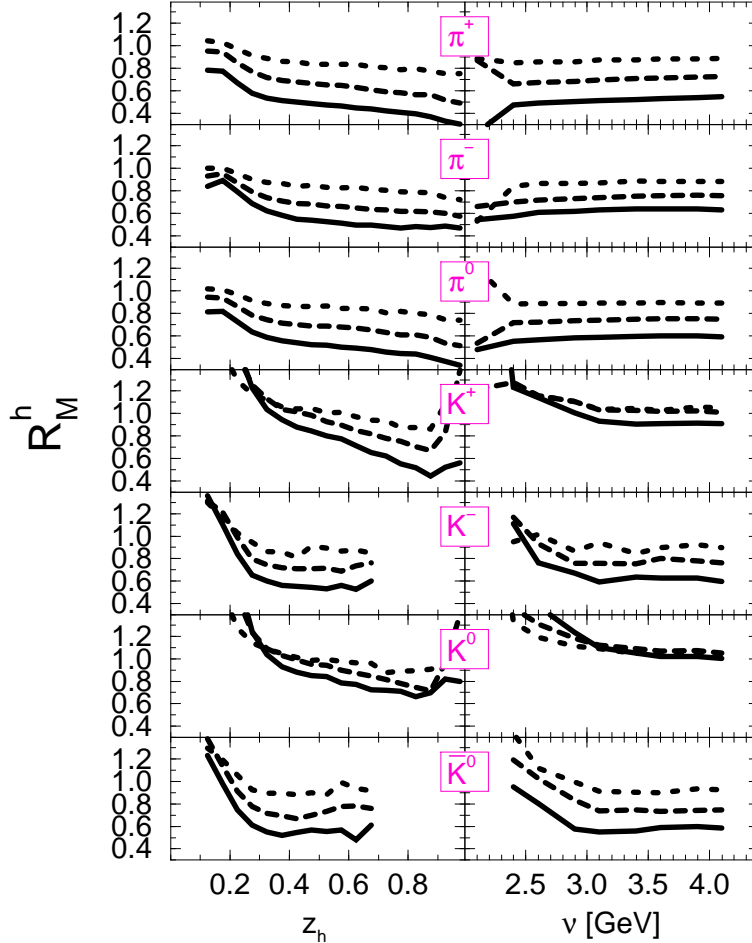


Fig. 6. Nuclear modification factor of identified mesons $\pi^{\pm,0}$ and $K^{\pm,0}, \bar{K}^0$ for JLAB(CLAS)@5GeV with different targets: ^{12}C (dotted), ^{56}Fe (dashed), ^{208}Pb (solid lines). Experimental acceptance limitations are taken into account (18)

comparison of our results (fig. 6) with preliminary experimental data on the z_h dependence of the π^+ attenuation for the three nuclear targets (20) is very satisfactory, both in its magnitude and its target mass number dependence.

Contrary to the situations at the higher beam energies, feeding effects leading to attenuation ratios larger than unity at small z_h are more pronounced and show up to be an essential feature at this energy. For the rarer kaons we stop showing the attenuation at $z_h = 0.7$ because the spectra for K^- drop rapidly at $z_h \approx 0.7 \dots 0.8$ as shown in fig. 7. On the contrary, the spectra for K^+ reach significantly farther out. This is a direct consequence of the fact that contrary to K^+ mesons the K^- mesons can only be produced in the associated

strangeness production mechanism and thus have a higher threshold than the former. The same holds for K^0 and \bar{K}^0 , respectively.

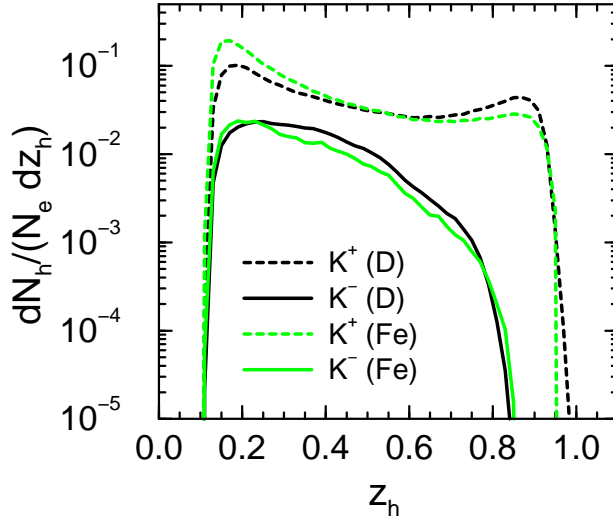


Fig. 7. z_h spectra of kaons/antikaons at JLAB@5GeV with D- and Fe-target.

At this low energy (and corresponding momentum transfer) the invariant masses populated in the first interaction are rather low ($\langle W \rangle = 2.2$ GeV) and thus just above the resonance region. We have also already noted that at this low energy we have formation times of only ≈ 4 fm at large z_h . Therefore, the interactions of the formed hadrons are strongly influenced by hadronic interactions with pre-hadronic interactions playing only a minor role, at least for the heavier targets. This shows up in fig. 6 in the different attenuation for K^+ and K^- , the latter being more strongly attenuated due to hadronic FSI. We also recall our earlier finding (10; 19) that at this low energy also effects of Fermi-motion are essential and have to be taken into account. The dynamics in this energy regime is thus more determined by 'classical' meson-nucleon dynamics than by perturbative QCD that underlies many of the other theoretical descriptions of the attenuation experiments (1; 12; 15).

Fig. 8 shows the calculated results for the multiplicity ratio of the three pion and four kaon species for the exemplary nuclei ^{12}C , ^{56}Fe and ^{208}Pb with 12 GeV lepton beam energy as for the future JLAB upgrade. For all particle species, a strong dependence of the attenuation ratios on the size of the nucleus is obtained. It is interesting to observe that at this higher energy the attenuation of K^+ and K^- is now similar at $z_h \approx 0.7$, contrary to the behavior at 5 GeV. This reflects the longer formation times at this higher energy and the corresponding predominance of pre-hadronic interactions which affect the K^- only weakly, these being non-leading hadrons.

A measurement of the z_h spectra of kaons would thus give interesting information on the production mechanism. We note that (21) have argued along

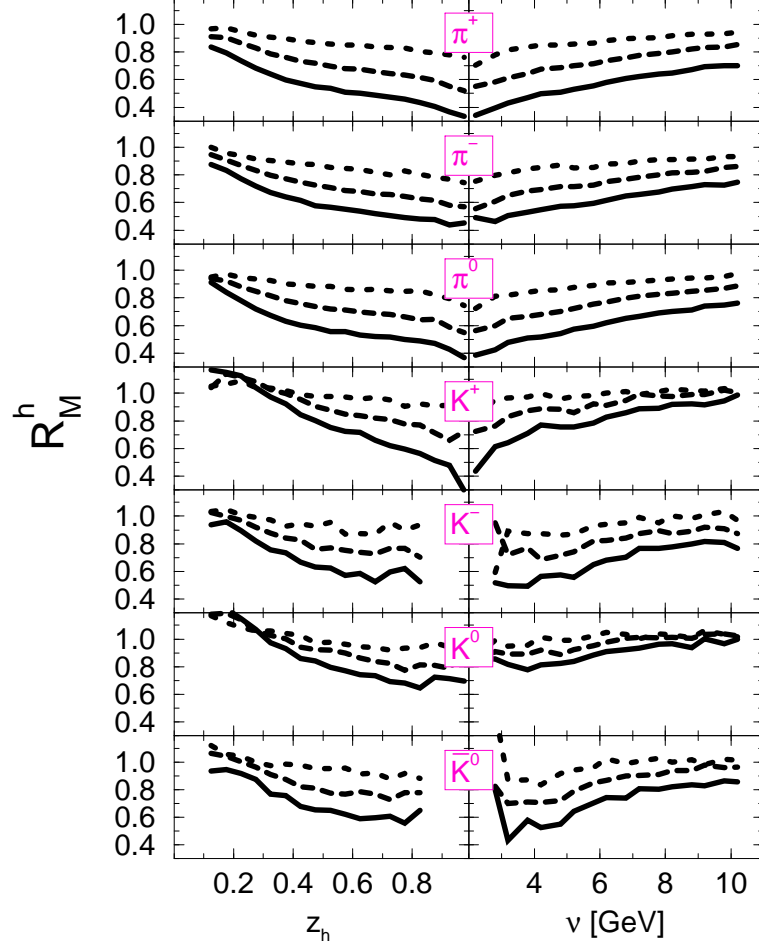


Fig. 8. Same as fig. 6, but now for JLAB(CLAS)@12GeV.

similar lines.

4 Conclusions

In the present work we have calculated hadron attenuation ratios for lepton induced reactions for the experimental conditions of the EMC and the HERMES collaboration with lepton beam energies varying from 280/100 GeV (EMC) to 27 GeV (HERMES). In addition, experimental conditions corresponding to HERMES at 12 GeV lepton beam energy and JLAB (CLAS) setups with 12 GeV and 5 GeV are considered. We present here a model based on (pre-)hadronic final state interactions, implemented via coupled channel transport equations, which covers the full energy range from 5 GeV up to several 100 GeV lepton beam energies and reproduces all available experimental data. The model now contains also the essential features of color transparency and should thus be suitable to analyze future experiments searching for this

phenomenon in hadron production experiments on nuclei.

The hard interactions are described by the string-breaking mechanism embedded in PYTHIA. Consistent with this mechanism hadron production and formation times are extracted from the full four dimensional information of the JETSET implementation of the Lund string fragmentation model.

The simultaneous description of the experimental data of the HERMES collaboration for 27 GeV and of the EMC collaboration for 100/280 GeV lepton beam energy requires a linear increase of the (pre-)hadronic cross section with time between the production and formation points. The measured attenuation data are indeed somewhat better described by pre-hadronic interactions that involve a Q^2 dependent pedestal value for the (pre-)hadronic cross section. The available data show only a weak sensitivity on Q^2 . This may also be due to the fact that at the higher energies most of the produced hadrons are non-leading so that they do not experience this Q^2 dependence that affects only the leading hadrons at large z_h . We, therefore, expect that this sensitivity becomes stronger at lower energies, because relatively more produced hadrons will be leading ones. However, at lower energies also the formation times become smaller and, therefore, the overall influence of the pre-hadronic interaction diminishes. In this sense the energy of 12 GeV, envisaged for the JLAB upgrade, may be a good compromise between the two competing effects. Some support for this expectation comes from our comparison of the K^+ and K^- attenuation. Here we have shown that at the lower energy of 5 GeV the attenuation of the former is much weaker than that of the latter because of the relatively short formation times and the corresponding dominance of hadronic interaction. At the higher energy of 12 GeV, however, the attenuation of the two becomes similar at large z_h because of the stronger influence of pre-hadronic interactions.

It will be interesting to analyze also reactions induced by pions ($\sqrt{s} \simeq 30$ GeV, Fermilab E706) or nucleons ($\sqrt{s} \simeq 20 \dots 200$ GeV, e.g. SPS, RHIC) to see if these reactions with hadronic entrance channels show a different behavior than the electromagnetic reactions analyzed in this paper (22).

5 Acknowledgments

This work has been supported by BMBF. The authors thank T. Falter for many lively discussions and his expertise, which found its way into the actual GiBUU code version. We appreciate the contributions of all members of the GiBUU team, especially O.Buss, T.Leitner, and J.Weil. We also gratefully acknowledge support by the Frankfurt Center for Scientific Computing.

References

- [1] B.Z. Kopeliovich et al., Nucl. Phys. A740 (2004) 211.
- [2] Y. Dokshitzer, V. Khoze, A. Mueller and S. Troyan, *Basics of perturbative QCD*, Editions Frontiers (1991).
- [3] K. Gallmeister, C. Greiner and Z. Xu, Phys. Rev. C67 (2003) 044905.
- [4] W. Cassing, K. Gallmeister and C. Greiner, Nucl. Phys. A735 (2004) 277.
- [5] G. R. Farrar, H. Liu, L. L. Frankfurt, M. I. Strikman, Phys. Rev. Lett. 61 (1988) 686.
- [6] A. Larson, G.A. Miller and M. Strikman, Phys. Rev. C74 (2006) 018201.
- [7] T. Sjöstrand et al., Comp. Phys. Commun. 135 (2001) 238;
T. Sjöstrand, L. Lönnblad and S. Mrenna, LU TP 01-21, hep-ph/0108264.
- [8] T. Falter, W. Cassing, K. Gallmeister, U. Mosel, Phys. Lett. B594 (2004) 61.
- [9] T. Falter, W. Cassing, K. Gallmeister, U. Mosel, Phys. Rev. C70 (2004) 054609.
- [10] T. Falter, Ph.D. Thesis, University of Giessen, 2004,
http://theorie.physik.uni-giessen.de/documents/dissertation/falter_phd.pdf
- [11] K. Gallmeister and T. Falter, Phys. Lett. B630 (2005) 40.
- [12] B.Z. Kopeliovich, J. Nemchik and I. Schmidt, Nucl. Phys. A782 (2007) 224.
- [13] <http://GiBUU.physik.uni-giessen.de>
- [14] B.Z. Kopeliovich and B.G. Zakharov, Phys. Rev. D44 (1991) 3466.
- [15] E. Wang and X.N. Wang, Phys. Rev. Lett. 89 (2002) 162301.
- [16] HERMES, P. van der Nat, Master Thesis, Amsterdam, 2002.
HERMES, A. Airapetian et al., Eur. Phys. J. C20 (2001) 479.
HERMES, G. Elbakyan, Proceedings of DIS2003, St. Petersburg.
HERMES, A. Airapetian et al., Phys. Lett. B577 (2003) 37.
HERMES, A. Airapetian et al., Nucl. Phys. B780 (2007) 1.
- [17] European Muon Collab, J. Ashman et al., Z. Phys. C52 (1991) 1.
- [18] W. Brooks, private communication, 2004
- [19] L. Alvarez-Ruso, T. Falter, U. Mosel and P. Muehlich, Prog. Part. Nucl. Phys. 55 (2005) 71.
- [20] CLAS, K. Hafidi, AIP Conf. Proc. 870 (2006) 669.
- [21] F. Arleo, Eur. Phys. J. C30 (2003) 213.
- [22] K. Gallmeister and U. Mosel, in preparation.